PHYSICAL REVIEW B VOLUME 31, NUMBER 6 15 MARCH 1985

Selective laser excitation of charge-compensated sites in KCl:Sm^{2+}

Albert J. Ramponi and John C. Wright
Department of Chemistry, University of Wisconsin—Madison, Madison, Wisconsin 53706
(Received 29 October 1984)

Site-selective laser spectroscopy is used to investigate the defect structure of KCl:Sm^{2+}. A total of nine sites have been identified at 12 K. Our results indicate that the C_{2v}[110] nearest-neighbor complex dominates the spectrum. All the other sites belong to clusters that can be eliminated by quenching from elevated temperatures. These clusters may represent the nucleation stage for the formation of the Suzuki phase. The overwhelming dominance of the C_{2v}[110] center is in disagreement with recent theoretical calculations which estimate the stability of the C_{2v}[110] and the C_{4v}[200] complexes to be comparable.

I. INTRODUCTION

The solid-state chemistry of alkali halide crystals intentionally doped with divalent cation impurities occupies a central position as models of point-defect equilibria and their relationship to measureable bulk properties. The nature of the local compensation in KCl:Sm^{2+} has been the subject of a number of different studies.[1–3] The aliovalent samarium ion, represented by $Sm_K^{\cdot}$ in the crystal, enters the KCl lattice substitutionally in place of a potassium ion, while a cation vacancy (V_K') is created for charge compensation. The different positions of the V_K' relative to the $Sm_K^{\cdot}$ gives rise to $Sm_K^{\cdot}$ sites with different point symmetries.[4] The formation of dimers, trimers, and higher order clusters of the $(Sm_K^{\cdot}\cdot V_K')^x$ pairs increases the number of possible sites, particularly at higher dopant concentrations.[5,6]

Bron and Heller[2] have performed a detailed study of the absorption and polarized emission of KCl:Sm^{2+}. They concluded that the dominant sharp line emission arises from a single nearest-neighbor complex possessing C_{2v} symmetry with the $Sm_K^{\cdot}$-V_K' axis lying along the [110] direction of the alkali halide lattice. This assignment was later disputed by Fong and Wong,[7] who claimed that C_{4v}[200]$(Sm_K^{\cdot}\cdot V_K')^x$ symmetry pairs accounted for some of the lines based on their studies of the first- and second-order Zeeman effect observed for this system. Fong[8] later showed that the calculated free energies of formation for the C_{2v}[110], C_{4v}[200], and C_s[211] site symmetries were all sufficiently close that each defect had observable concentrations which could be described by a Maxwell-Boltzmann distribution. In an extensive series of experiments Fong and co-workers[4,5,9–11] determined that some of the lines originally assigned to the C_{2v}[110] site could instead be assigned to sites with C_{4v}[200] and C_s[211] symmetry corresponding to vacancies in the next-nearest- and third-nearest-neighbor positions, respectively. Bradbury and Wong[12] later challenged this work and provided an alternative interpretation that reinforced the original assignment that all the dominant lines come from the C_{2v}[110] $(Sm_K^{\cdot}\cdot V_K')^x$ pair. Ford and Fong[13] and Heist, Chilver, and Fong[14] then argued that the lines at 728.28, 769.45, 813.26, and 819.47 nm did not come from the C_{2v}[110] site but were associated with sites of C_{4v}[200] and C_s[211] symmetry.

The experiments performed by these workers were difficult because each of the spectral lines had to be studied individually by a number of techniques in order to arrive at a site identification. The method of site-selective laser spectroscopy eliminates many of the problems encountered by previous investigators, because a single site can be selectively excited to obtain a single-site fluorescence spectrum or the fluorescence can be selectively monitored to obtain a single-site excitation spectrum. By repeating such experiments for all the excitation wavelengths and fluorescence transitions and by requiring that the relative intensities of transitions remain constant, the transitions common to a specific site can be determined unambiguously. In this paper, we report the results of site-selective laser spectroscopy for KCl:Sm^{2+}. We show that there are at least nine observable sites but that all the dominant transitions come from a single $(Sm_K^{\cdot}\cdot V_K')^x$ pair with C_{2v}[110] symmetry. This result is somewhat surprising because recent theoretical calculations[15] predict that the defect energies associated with the formation of the C_{2v}[110] and C_{4v}[200] sites for alkaline-earth cations in KCl are comparable. The other sites correspond to clusters that can be eliminated by quenching from elevated temperatures. These clusters may represent the nucleation stage for the formation of separate Suzuki-type phases which have been observed in KCl crystals doped with divalent europium.[16] This study shows that the solid-state defect equilibria in KCl:Sm^{2+} are particularly simple since all of the isolated divalent samarium ions are locally compensated by a cation vacancy in the nearest-neighbor [110] position.

II. EXPERIMENTAL METHODS

A pulsed nitrogen laser operated at 400-kW peak power with a 10-ns pulse width pumps a tunable dye laser that has a measured bandwidth of approximately 0.02 nm. The dye-laser beam is focused onto the sample which is attached to the cold finger of a cryogenic refrigerator system capable of temperatures between 12—300 K. Experi-

ments were also conducted at 4.2 and 2.2 K with a liquid-helium Dewar. Unless otherwise specified the sample temperature was approximately 12 K.

Fluorescence from the sample is dispersed using either a low-resolution 0.25-m Fastie-Ebert monochromator or a high-resolution 1-m Czerny-Turner monochromator, depending upon whether individual fluorescence lines need to be observed. A gated integrator is used to detect the signal of interest. The fluorescence relaxation was measured with a transient recorder interfaced to a Digital Equipment Corporation PDP8/f microcomputer for signal averaging. A detailed description of the selective-laser-excitation technique and apparatus is published elsewhere.[17]

The samples used in this study are single crystals grown from the melt by the Czochralski method at a Sm^{2+} dopant concentration of approximately 0.01 mol% as determined by neutron activation analysis. Thermal annealing experiments were performed under vacuum (10^{-5} Torr) or HCl gas at 250 Torr by sealing the crystals inside a Vycor tube. The ampoule was placed in a tube furnace, heated to 650°C for 24 h, and then rapidly quenched by direct immersion into ice water.

III. RESULTS

The Sm^{2+} ion has $^5D_0$ and $^5D_1$ excited states in the $4f^6$ electron configuration and slightly higher bands belonging to the $4f^5 5d^1$ configuration that can be excited with a dye laser. Fluorescence occurs from the $^5D_0$ level to lower states in the ^7F_J multiplet. The excitation spectrum for the $^7F_0 \rightarrow {}^5D_0$ transition monitoring fluorescence at 726.5 nm with a 6.6-nm bandpass appears in Fig. 1 with two different gate widths for the gated detection. Each line appearing in the spectrum corresponds to a unique crystallographic center because the $^7F_0 \rightarrow {}^5D_0$ transition can have only one line per site. A letter is associated with each line for organizational purposes. Site a gives rise to the dominant sharp line emission corresponding to the $C_{2v}[110]$ site. Sites g through j appear enhanced in Fig. 1(a) because the wavelength selected and the short delay and gate width for the gated integrator favor these sites. Figure 1(b) was obtained with a longer gate to reflect the total relative intensities of lines with different lifetimes. The $C_{2v}[110]$ line is particularly dominant. Additional, less intense absorptions near site g are visible for excitation scans performed at higher resolution using the 1-m monochromator monitoring fluorescence at 727.88 nm. These sites are labeled ϵ and h and appear in the inset of Fig. 1(a). Expanded scans across the excitation line at 691.27 nm (site j) reveal that it is composed of a family of sites and quite possibly represents a continuum of sites (*vide infra*).

Fluorescence spectra from individual sites can be obtained by tuning the laser to resonance with each line in Fig. 1. In turn, single-site excitation spectra can be examined by setting the 1-m monochromator to successive lines in the fluorescence spectra and scanning the dye laser over the possible excitation regions. As already mentioned, laser excitation corresponding to $^7F_0 \rightarrow {}^5D_0$ at 689.19 nm (site a in Fig. 1) selectively gives rise to the dominant line

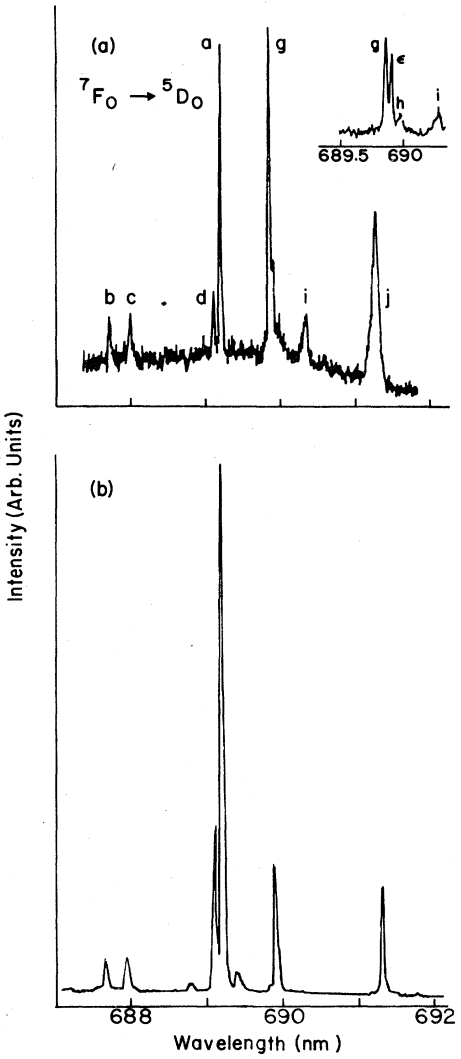

FIG. 1. $^7F_0 \rightarrow {}^5D_0$ excitation spectrum monitoring all fluorescence at 726.5 nm. (a) Delay equals 40 μs, gate equals 1 ms. The inset shows a high-resolution scan near site g, monitoring fluorescence at 727.88 nm. (b) Delay equals 50 μs, gate equals 5 ms.

emission. Excitation of the $^5D_1$ level results in rapid nonradiative decay to the $^5D_0$ level with subsequent radiative relaxation to the ground state. Figure 2 shows the $^5D_0 \rightarrow {}^7F_J (J=0\text{–}4)$ fluorescence spectrum resulting from laser excitation at 636.90 nm of the $^5D_1$ level. The relative intensities are the same as those observed by exciting at 689.19 nm in $^5D_0$ but the absolute intensity of all the lines is considerably stronger when the $^5D_1$ manifold is excited. Furthermore, the lines in these spectra exactly match the dominant line emission discussed in the literature for the $C_{2v}[110]$ site. The fluorescence wavelengths and energies for all the measurable sites are tabulated in Table I, where they are grouped according to the terminal state of the fluorescence. Regardless of the excitation wavelength in the $^7F_0 \rightarrow {}^5D_1$ region, the $C_{2v}[110]$ emis-

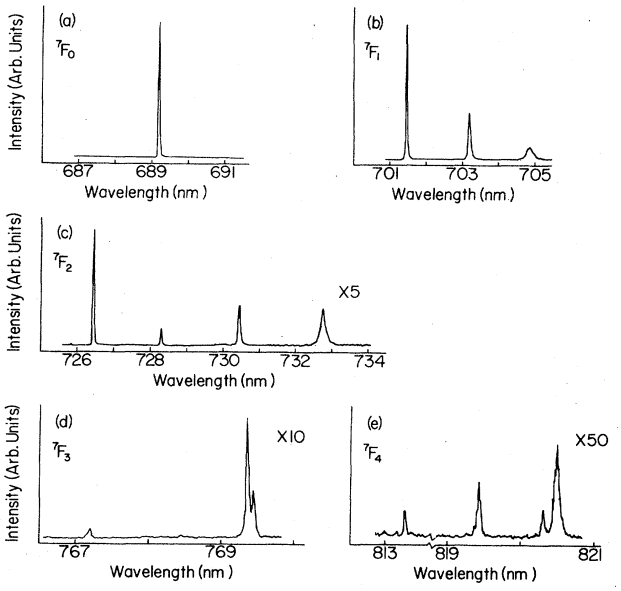

FIG. 2. $^5D_0 \rightarrow {}^7F_J(J=0\text{—}4)$ fluorescence spectrum for site a exciting at 636.90 nm in $^5D_1$.

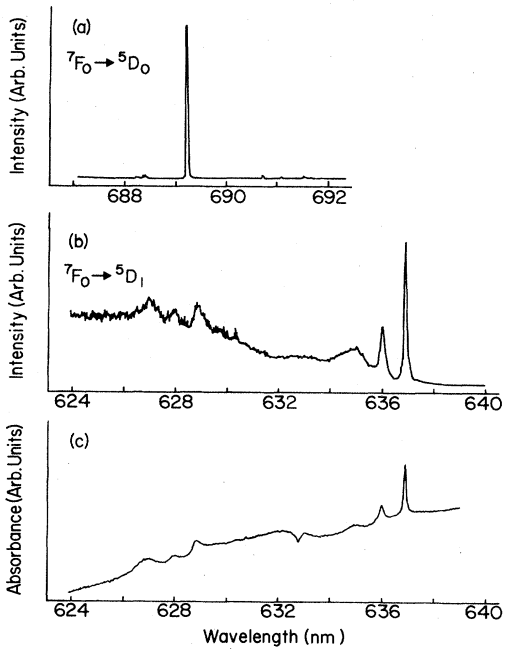

FIG. 3. (a) $^7F_0 \rightarrow {}^5D_0$ excitation spectrum for site a monitoring 701.47 nm. (b) $^7F_0 \rightarrow {}^5D_1$ excitation spectrum for site a monitoring 689.19 nm. (c) Broad-band absorption spectrum for $^5D_1$ level at 12 K.

sion spectrum is observed with the same line positions and relative intensities. Careful measurements were made of the relative intensities for the 728.28-, 769.45-, 813.26-, and 819.47-nm lines that were assigned to $C_{4v}[200]$ and $C_s[211]$ site symmetries by Hiest, Chilver, and Fong.[14] As would be expected for fluorescent lines arising from a single site, these transitions always have the same relative intensities to all the other lines belonging to site a within experimental error (10%) regardless of the excitation wavelength. The $^7F_0 \rightarrow {}^5D_0$ and $^7F_0 \rightarrow {}^5D_1$ excitation spectra monitoring 701.47 and 689.19 nm, respectively, are shown in Figs. 3(a) and 3(b). The same excitation profiles were observed for each of the emission lines associated with this site. The absorption spectrum obtained with a tungsten lamp of the $^5D_1$ region at 12 K appears in Fig. 3(c) for comparison. The similarities between Figs. 3(b) and 3(c) are obvious and suggest that any absorption in the $^5D_1$ region will preferentially give rise to the $^5D_0 \rightarrow {}^7F_J$ fluorescence belonging to the $C_{2v}[110]$ site as we have observed. The broad structure in Figs. 3(b) and 3(c) is due to the onset of absorption from the $4f^5 5d^1$ bands. The reproducible dip in the absorption spectrum at 632.80 nm in Fig. 3(c) is thought to be a Fano antiresonance[18] arising from a strong coupling between the $4f^5 5d^1$ and $4f^6$ electron configurations in this wavelength region.

The fluorescence intensity from individual sites can have a strong dependence on the sample temperature. The fluorescence from the $C_{2v}[110]$ site for example is quenched as the crystal temperature is raised to 12 K. Another site labeled k is so strongly quenched that it cannot be observed at 12 K and measurements are best made at liquid-helium temperatures. Figures 4(a)—4(c) show the $^5D_0 \rightarrow {}^7F_J(J=0\text{—}2)$ fluorescence spectrum obtained at 2.2 K for laser excitation at 641.06 nm of the $^5D_1$ manifold. This laser wavelength selectively excites fluorescence from sites k and g simultaneously, but also excites some fluorescence from the $C_{2v}[110]$ site. At 2.2 K, sites a and k dominate the spectrum. Note that the line at 703.17 nm in $^7F_1$ [Fig. 4(b)] which belongs to the $C_{2v}[110]$ site overlaps a transition from site k. The wavelengths for the $^5D_0 \rightarrow {}^7F_J(J=0\text{—}2)$ transitions corresponding to site k are listed in Table I. Sites with strong temperature-dependent quenching are attributed to thermal population of nearby levels from the $4f^5 5d^1$ configuration.[19]

The $^7F_0 \rightarrow {}^5D_0$ excitation and $^5D_0 \rightarrow {}^7F_{1,2}$ fluorescence spectra for the remaining sites are shown in Fig. 5. The transitions observed for each site are included in Table I. In most cases it is possible to obtain fluorescence spectra characteristic only of the site of interest, but it is not possible to obtain single-site excitation spectra because of spectral overlap with other sites. Site assignments were made only after observing the same transitions with the same relative intensities for no less than three different fluorescence wavelengths. In cases where overlap of fluorescence lines produces contributions from more than one site in excitation, the line assignment is indicated in Fig. 5. Fluorescence spectra are not shown for the higher ^7F_J manifolds due to the presence of an intense short-lived background emission which interferes with fluorescence to the higher manifolds making peak assignments in this region difficult for the short-lived sites. The lifetimes of the $^5D_0$ level for the most intense sites are listed in Table II. The $^5D_0$ fluorescence decay time for sites a and k were measured at 2.2 K due to the strong temperature-

TABLE I. Fluorescence transitions for the individual Sm^{2+} sites in KCl. The transition energies have been corrected to vacuum.

Transition	Site	Wavelength (nm)	Energy (cm^{-1})	Transition	Site	Wavelength (nm)	Energy (cm^{-1})
$^5D_0 \rightarrow {}^7F_0$	b	687.71	14 537.0	$^5D_0 \rightarrow {}^7F_2$	b	727.48	13 742.3
	c	687.99	14 531.1	(Cont'd.)	c	727.83	13 735.7
	l[a]	688.87	14 512.5		ϵ	727.88	13 734.7
	d	689.10	14 507.7		k	727.90	13 734.4
	a	689.19	14 505.8		k	728.03	13 731.9
	g	689.85	14 491.9		l	728.16	13 729.5
	ϵ	689.91	14 490.6		a	728.28	13 727.2
	k[b]	689.91	14 490.6		d	728.43	13 724.4
	i[c]	690.34	14 481.6		b	728.65	13 720.2
	j[d]	691.27	14 462.1		c	728.98	13 714.0
					b	729.65	13 701.4
$^5D_0 \rightarrow {}^7F_1$	m[a]	698.73	14 307.7		l	729.85	13 697.7
	a	701.47	14 251.8		d	729.97	13 695.4
	d	701.80	14 245.1		c	730.01	13 694.7
	l	701.82	14 244.7		a	730.46	13 686.2
	d	702.26	14 235.8		g	731.44	13 667.9
	g	702.70	14 226.9		g	731.75	13 662.1
	?[e]	703.01	14 220.6		l	731.79	13 661.4
	ϵ	703.15	14 217.8		k	732.05	13 656.5
	k	703.16	14 217.6		d	732.19	13 653.9
	a	703.17	14 217.4		g/ϵ	732.33	13 651.3
	ϵ	703.49	14 210.9		a	732.76	13 643.3
	g	703.51	14 210.5		ϵ	732.81	13 642.3
	ϵ	703.93	14 202.0				
	k	703.99	14 200.8	$^5D_0 \rightarrow {}^7F_3$	l	766.99	13 034.4
	k	704.39	14 192.8		a	767.19	13 031.0
	a	704.82	14 184.1		l	768.98	13 000.7
	d	705.16	14 177.3		l	769.07	13 099.1
	l	705.35	14 173.4		a	769.35	12 994.4
					a	769.45	12 992.7
$^5D_0 \rightarrow {}^7F_2$	b	724.94	13 790.4	$^5D_0 \rightarrow {}^7F_4$	l	812.71	12 301.1
	c	725.23	13 784.9		a	813.26	12 292.8
	l	726.00	13 770.3		l	818.97	12 207.1
	d	726.27	13 765.2		a	819.47	12 199.6
	a	726.44	13 762.0		l	820.03	12 191.3
	g	726.87	13 753.8		a	820.31	12 187.2
	ϵ	727.36	13 744.6		a	820.49	12 184.5
	g	727.45	13 742.9				

[a]Site l appears in sample annealed under HCl.
[b]Site k is observed for $T \leq 4.2$ K.
[c]Fluorescence from site i was not observed.
[d]Site j represents a continuum of sites (see text).
[e]Origin unknown but appears in fluorescence spectrum for site g.

dependent quenching of these sites at higher temperatures. All other measurements were made at 12 K. Sites a through d and site k have distinct fluorescence patterns and also possess long lifetimes for the $^5D_0$ level. The excitation spectra for sites b and c show a contribution from site a [Figs. 5(a) and 5(b)] because of spectral overlap with the much higher site concentration of the C_{2v}[110] center. The excitation spectrum of site b also has a minor contribution from site c but the spectral characteristics of the individual sites are still distinguishable. The lines of the $^5D_0 \rightarrow {}^7F_2$ transition for sites b and c are very similar except for the small offset. Since this offset is identical to that of the $^7F_0 \rightarrow {}^5D_0$ transitions, the shift corresponds to differences in the position of the $^5D_0$ level. Unlike site d, however, neither center shows appreciable fluorescence in the $^5D_0 \rightarrow {}^7F_1$ transition.

The remaining sites possess lifetimes for $^5D_0$ that are less than 15 μs. These short-lived sites are more difficult to characterize due to broad background emission and overlapping fluorescence. For example, Figs. 5(d) and 5(e) show the fluorescence arising from sites g and ϵ, respectively. Extensive spectral overlap in both the $^7F_1$ and $^7F_2$

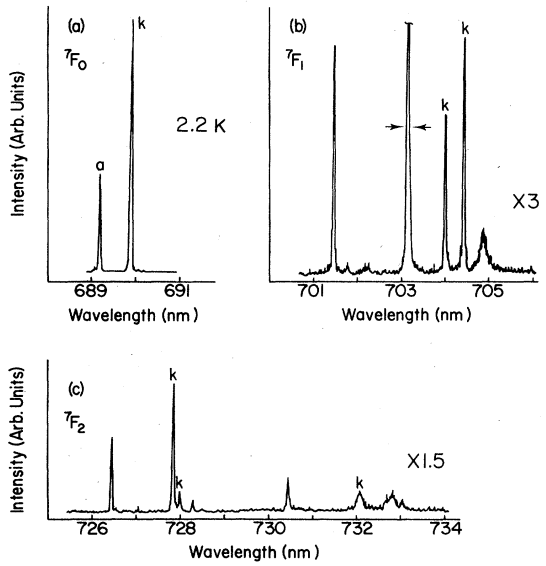

FIG. 4. $^5D_0 \rightarrow {}^7F_J(J=0-2)$ fluorescence spectrum at 2.2 K for site k exciting at 641.06 nm in $^5D_1$. This excitation wavelength also excites fluorescence from sites g and a.

TABLE II. Fluorescence lifetime of the $^5D_0$ level for the Sm^{2+} sites. The values in parentheses represent the percent error associated with the reported value. Sample temperature was 12 K unless otherwise specified.

Site	Lifetime (ms)
a	10.58 (0.8)[a]
b	2.01 (5.6)
c	1.81 (4.0)
d	8.05 (1.1)
g	$\lesssim 0.01$
ϵ	<0.01
j	<0.01[b]
k	5.99 (11)[a]
l	8.18 (2.2)[c]

[a]Measured at 2.2 K.
[b] Value is representative for all sites collectively called site j (see text).
[c]Site l appears in sample annealed under HCl.

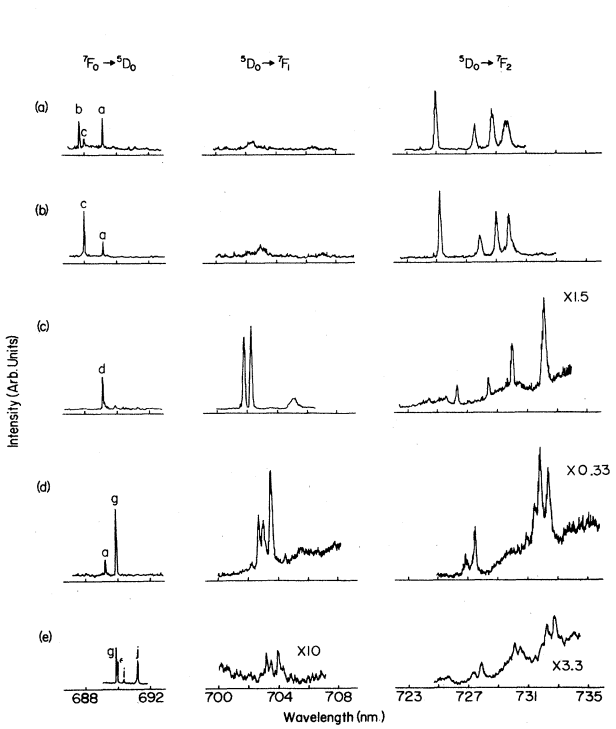

FIG. 5. $^7F_0 \rightarrow {}^5D_0$ excitation and $^5D_0 \rightarrow {}^7F_{1,2}$ fluorescence spectra for the remaining sites. Transitions that are present from interfering sites in excitation are indicated in the spectra. (a) Site b; monitoring 729.65 nm for excitation, exciting at 687.71 nm for fluorescence. (b) Site c; monitoring 725.23 nm, exciting 687.99 nm. (c) Site d; monitoring 702.26 nm, exciting 689.10 nm. (d) Site g; monitoring 703.51 nm, exciting 689.85 nm. (e) site ϵ; monitoring 732.33 nm, exciting 689.91 nm.

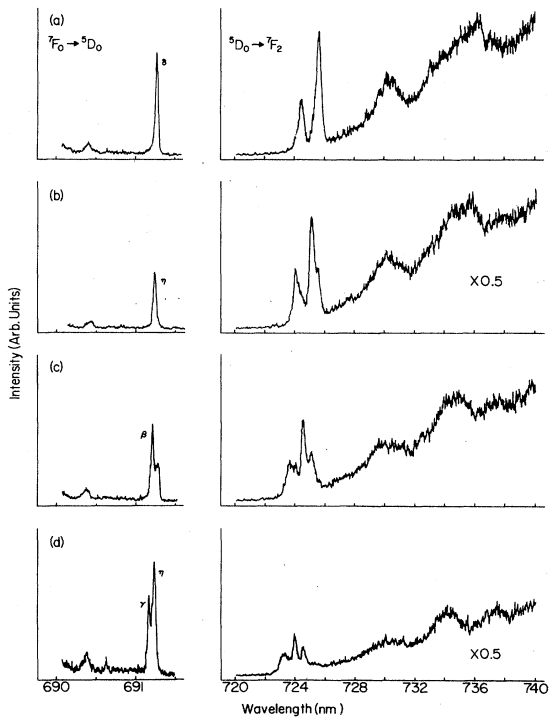

FIG. 6. $^7F_0 \rightarrow {}^5D_0$ excitation and $^5D_0 \rightarrow {}^7F_2$ fluorescence spectra for the family of sites collectively referred to as site j. Transitions that are present from interfering sites in excitation are indicated in the spectra. (a) Site δ; monitoring 725.515 nm for excitation, exciting at 691.278 nm for fluorescence. (b) Site η; monitoring 724.940 nm, exciting 691.233 nm. (c) site β; monitoring 724.503 nm, exciting 691.208 nm. (d) site γ; monitoring 723.873 nm, exciting 691.196 nm.

regions result in excitation spectra that cannot be completely resolved for either site. However, the superior intensity of site g relative to site ϵ makes the fluorescence spectral assignment much easier for this site. The difficulty in completely characterizing site ϵ can be appreciated by observing the excitation spectrum [Fig. 5(e)] which, although optimized for site ϵ, remains dominated by site g.

The crystallographic center referred to as site j in Fig. 1(a) is actually a composite of no less than four closely spaced sites. The $^7F_0 \rightarrow {}^5D_0$ excitation and $^5D_0 \rightarrow {}^7F_2$ fluorescence spectra for this family of sites are compared in Fig. 6. Fluorescence corresponding to $^5D_0 \rightarrow {}^7F_1$ was not observed for any of these sites. Spectral congestion in the $^7F_2$ region makes it difficult to isolate a single fluorescence line indicative of an individual site. Nevertheless comparatively large fluorescence line shifts are observed in response to small changes in the excitation wavelength. A series of scans done at approximately 0.025-nm increments of the dye laser shows that the fluorescence lines do not shift continuously in the manner observed for fluorescence line narrowing of an inhomogeneous line,[20] but instead rise and fall in intensity at a constant monochromator wavelength. This behavior is consistent with a finite number of different sites making up the line initially labeled site j.

With the exception of site g, site-selective excitation of the $^7F_0 \rightarrow {}^5D_1$ transition could not be easily realized for the other sites since partial overlap of the $^5D_1$ level with the $4f^5 5d^1$ band results in efficient excitation of the $^5D_0$ level for the $C_{2v}[110]$ site. Thus the fluorescence from the other sites was either very weakly observed or completely obscured for this region.

Annealing experiments were performed under vacuum to observe the changes in the site distribution when a crystal is rapidly quenched from 650 °C. All of the sites except the $C_{2v}[110]$ center decreased markedly in importance to the point where most could not be detected. This behavior has previously been observed by Heist, Chilver, and Fong,[14] and suggests that all the other sites are associated with clustering of multiple Sm^{2+} ions together with their charge-compensating cation vacancy. Based on entropy considerations, single $(Sm_K \cdot V_K)^x$ pairs other than the $C_{2v}[110]$ pair would be favored by high-temperature quenching as shown by Fong, Ford, and Heist.[21] It is particularly important to note that all of the fluorescence lines shown in Fig. 2 for the $C_{2v}[110]$ site, including the lines at 728.28, 769.45, 813.26, and 819.47 nm, which have been assigned[14] to $C_{4v}[200]$ and $C_s[211]$ sites, maintain the same relative intensities within experimental error (9%) for the annealed crystal.

A second annealing experiment was performed for a crystal that was encapsulated under approximately 250 Torr of HCl before being heated and quenched from 650 °C. The crystal was bleached after annealing and excitation of the $4f^5 5d^1$ bands with a nitrogen laser ($\lambda = 337.1$ nm) gave rise to the fluorescence spectra shown in Fig. 7 for the $^5D_0 \rightarrow {}^7F_J (J = 0\text{–}4)$ transitions. In addition to the transitions belonging to the $C_{2v}[110]$ center, a number of new lines appear in these spectra, with two sites labeled l and m accounting for the additional transitions as indicated in Fig. 7 and Table I. Fluorescence line assignments are based on lifetime measurements and line-intensity variations with crystal temperature. Site l possesses a relatively weak thermal dependence compared to either site m or the $C_{2v}[110]$ center. The lifetime of the $^5D_0$ level for site l is included in Table II. Weak $^5D_0 \rightarrow {}^7F_{1,2}$ fluorescence was detected for site l and the $C_{2v}[110]$ site for selective $^7F_0 \rightarrow {}^5D_0$ excitation. The very low intensity observed for selective excitation of any of the sites clearly indicates that there has been a drastic change in the site concentrations. Nevertheless, there is no change in the relative intensity among the transitions that have been assigned to the $C_{2v}[110]$ site.

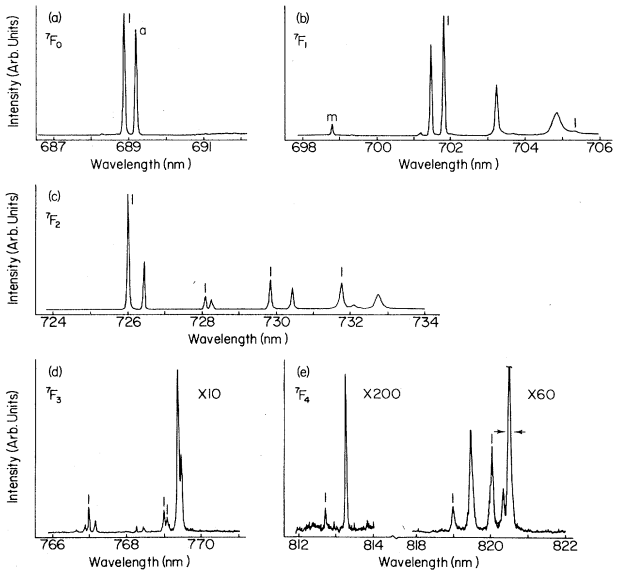

FIG. 7. $^5D_0 \rightarrow {}^7F_J (J = 0\text{–}4)$ fluorescence spectrum for crystal annealed under HCl ($\sim$250 Torr) exciting at 337.1 nm in the $4f^5 5d^1$ bands.

IV. DISCUSSION AND CONCLUSIONS

These experiments have shown that the $C_{2v}[110]$ center is the only simple $(Sm_K \cdot V_K)^x$ single pair site that is important in KCl:0.01 mol % Sm^{2+}. EPR experiments performed by Watkins[22] on KCl:Mn^{2+} and theoretical calculations performed by several workers[15,21,23] on similar systems suggest that the $C_{2v}[110]$ site is not the only dominant associated-pair site. Recently, Catlow, Corish, Quigley, and Jacobs[15] have used computer models to calculate the defect energies for alkaline-earth cations in KCl and other alkali halide hosts. Their results predict that the $C_{2v}[110]$ and $C_{4v}[200]$ sites should both be important, with the $C_{2v}[110]$ site dominating for cations with large ionic radii and the $C_{4v}[200]$ site for small cations. The ionic radii of Sm^{2+} and Sr^{2+} differ by only 2%. Based solely on the ionic radii of Mn^{2+} and Sm^{2+}, one can estimate the binding energies for each dipolar complex by interpolation from the results of the theoretical modeling. The Mn^{2+} ion would then have binding ener-

gies of -0.60, -0.63, and -0.34 eV for the $C_{2v}[110]$, $C_{4v}[200]$, and $C_s[211]$ sites, respectively, while Sm^{2+} would have binding energies of -0.65, -0.60, and -0.37 eV. It should be emphasized that these estimates ignore important physical properties of the dopant ion which determine covalent and other ion specific interactions. In particular, the short-range potentials between the dopant ion and the host lattice and the dopant ion polarizability are two quantities that can significantly alter the results of the modeling.[24] Nevertheless the binding energies obtained from EPR measurements on KCl:Mn^{2+} are consistent with this oversimplified approach since the $C_{2v}[110]$ and $C_{4v}[200]$ sites are both prominent although the absolute values measured experimentally are -0.39 and -0.42 eV, respectively.[22] Our results, however, are inconsistent with these estimates of the binding energies for KCl:Sm^{2+}. Although the calculations indicate the correct trend toward greater dominance of the $C_{2v}[110]$ site with larger ionic radius, the relative differences in the binding energies are not large enough to account for the overwhelming dominance of the $C_{2v}[110]$ site. However, Nunes, Souza, and Castro[25] have performed experiments using two-photon absorption spectroscopy in which they observed both the $C_{2v}[110]$ and $C_{4v}[200]$ sites in KCl:Eu^{2+}. The appearance of the $C_{4v}[200]$ site is surprising due to the similarity of both systems.

The possibility that the $C_{4v}[200]$ site is present only at ordinary temperatures was investigated by rapidly quenching a sample from room temperature to 4.2 K. The jump rate of a cation vacancy associated with a nearest-neighbor divalent impurity is given by

$$\nu = 12\nu_0 \exp(-\epsilon/kT) , \tag{1}$$

where ν_0 is called the frequency factor [$\nu_0 \simeq 0.25\times 10^{14}$ sec^{-1} for KCl (Ref. 26)], ϵ is the cation vacancy-impurity association energy estimated to be 0.7 eV,[26] and T is the equilibrium site-distribution temperature. By requiring that the change in the jump rate be less than the rate of cooling for a given time interval, we estimate an equilibrium site-distribution temperature of $T\sim 250$ K for a sample that is quenched from room temperature to 4.2 K. Even under these conditions, the relative site distribution resulting from nitrogen-laser excitation of the $4f^5 5d^1$ band shows no evidence of the $C_{4v}[200]$ complex and appears identical to that observed under normal sample cooldown which proceeds much more slowly.

The difference in the binding energies of the $C_{2v}[110]$ and $C_{4v}[200]$ complexes can be estimated from the following expression:[22]

$$n_1/n_2 = \tfrac{12}{6}\exp(\Delta\epsilon/kT) , \tag{2}$$

where n_1/n_2 is the ratio of the $C_{2v}[110]$ to $C_{4v}[200]$ complexes at the equilibrium distribution temperature, $\Delta\epsilon=\epsilon_1-\epsilon_2$ represents the difference in binding energies of the two sites, and $\frac{12}{6}$ is the ratio of available positions about the divalent impurity for the $C_{2v}[110]$ and $C_{4v}[200]$ complexes. Using our data from the quenched crystal, we conservatively estimate $n_1/n_2\sim 456$ from the signal-to-noise ratio for the line at 689.19 nm of the $C_{2v}[110]$ site. Therefore, the difference in binding energies of the $C_{2v}[110]$ and $C_{4v}[200]$ complexes is no smaller than 0.12 eV. A significant contribution from the $C_{4v}[200]$ site has recently been suggested[15] to explain discrepancies between theoretical and experimental diffusion measurements of divalent cation impurities in the alkali halides. The contribution from $C_{4v}[200]$ dipolar complexes to diffusion kinetics was used to explain differences of approximately 0.8 and 0.4 eV between experimental migration energies and theoretical calculations for the KCl:Ca^{2+} and KCl:Sr^{2+} systems, respectively. If the isolated $(Sm_K\cdot V_K)^x$ point symmetry is representative of the impurity-vacancy pair orientation for the alkaline earth cations in KCl, the observation of only a $C_{2v}[110]$ site would argue that other factors must be responsible for the disagreements.

The $^7F_0\rightarrow{}^5D_0$ excitation spectrum [Fig. 1(a)] taken with a short gate width shows prominent lines labeled g, i, and j which are assigned to clusters containing multiple Sm^{2+} ions. These sites have much shorter lifetimes than the other sites. The short lifetimes are attributed to quenching processes and not to enhanced radiative transition rates. Although the radiative rate can be increased by configurational mixing with a nearby $4f^5 5d^1$ band as observed in CaF_2:Sm^{2+},[27] there is no evidence that the $4f^5 5d^1$ band plays an important role for the g, i, and j sites. Thermal quenching via transfer to the $4f^5 5d^1$ band is not efficient nor does excitation above the $^5D_0$ energy level cause appreciable fluorescence from these sites as would be observed if the $4f^5 5d^1$ band was nearby. Quenching of these sites could occur by energy-transfer processes if the sites belong to the precipitated Suzuki phase commonly observed in heavily doped crystals.[28] The energy levels of Sm^{2+} do not have proper energy matches to permit efficient two-body transfer,[29] but the rapid excitation migration to sinks which is observed in concentrated materials could cause the quenching[30]

The strong quenching will make the integrated intensity in a fluorescent transient from the g, i, and j sites low but the initial peak intensities should not be affected by the quenching since they depend upon the initial excited-state population and the radiative decay rate. Excitation spectra taken with short gate widths would better represent the relative concentrations of the different sites. Thus the g, i, and j sites are believed to represent substantial concentrations and most likely correspond to the sites that are responsible for the changes in the uv-absorption spectra observed by Rubio, Murrieta, Hernández, and López[16] in KCl:Eu^{2+}. These changes were attributed to the formation of the Suzuki phase as well as three other phases associated with Eu^{2+} precipitation. The g, i, and j sites can therefore be used to resolve the details of how these phases form.

ACKNOWLEDGMENTS

The authors wish to express their gratitude to Dr. F. K. Fong and Dr. R. H. Heist, who kindly provided the crystals used in these experiments. This work was supported by the National Science Foundation under Grant No. DMR-82-05145.

[1]A. A. Kaplyanskii and P. P. Feofilov, Opt. Spectrosc. **16**, 144 (1964).
[2]W. E. Bron and W. R. Heller, Phys. Rev. **136**, A1433 (1964).
[3]F. K. Fong and E. Y. Wong, in *Optical Properties of Ions in Crystals,* edited by H. M. Crosswhite and H. W. Moos (Wiley, New York, 1967), p. 137.
[4]F. K. Fong, M. N. Sunberg, R. H. Heist, and C. R. Chilver, Phys. Rev. B **3**, 50 (1971).
[5]F. K. Fong, R. H. Heist, C. R. Chilver, J. C. Bellows, and R. L. Ford, J. Lumin. **2**, 823 (1970).
[6]S. L. Naberhuis and F. K. Fong, J. Chem. Phys. **56**, 1174 (1972).
[7]F. K. Fong and E. Y. Wong, Phys. Rev. **162**, 348 (1967).
[8]F. K. Fong, Phys. Rev. **187**, 1099 (1969).
[9]F. K. Fong, Phys. Rev. B **1**, 4157 (1970).
[10]F. K. Fong and J. C. Bellows, Phys. Rev. B **1**, 4240 (1970).
[11]F. K. Fong and J. C. Bellows, Phys. Rev. B **2**, 2636 (1970).
[12]R. E. Bradbury and E. Y. Wong, Phys. Rev. B **4**, 690 (1971); **4**, 694 (1971); **4**, 702 (1971).
[13]R. L. Ford and F. K. Fong, J. Chem. Phys. **56**, 1972 (1972).
[14]R. H. Heist, C. R. Chilver, and F. K. Fong, Phys. Rev. B **5**, 4237 (1972).
[15]C. R. A. Catlow, J. Corish, J. M. Quigley, and P. W. M. Jacobs, J. Phys. Chem. Solids **41**, 231 (1980).
[16]F. J. López, H. Murrieta S., J. Hernández A., and J. Rubio O., Phys. Rev. B **22**, 6428 (1980); J. Rubio O., H. Murrieta S., J. Hernández A., and F. J. López, *ibid.* **24**, 4847 (1981).
[17]M. P. Miller, D. R. Tallant, F. J. Gustafson, and J. C. Wright, Anal. Chem. **49**, 1474 (1977).
[18]See for example, J. P. van der Ziel and L. G. Van Uitert, Phys. Rev. B **8**, 1835 (1973).
[19]M. Guzzi and G. Baldini, J. Lumin. **6**, 270 (1973).
[20]A. Szabo, Phys. Rev. Lett. **25**, 924 (1970).
[21]F. K. Fong, R. L. Ford, and R. H. Heist, Phys. Rev. B **2**, 4202 (1970).
[22]G. D. Watkins, Phys. Rev. **113**, 79 (1959).
[23]M. P. Tosi and G. Airoldi, Nuovo Cimento **8**, 584 (1958).
[24]J. M. Quigley (private communication).
[25]Luiz A. O. Nunes, Gabriel P. Souza, and Jarbas C. Castro, in the proceedings from the International Conference on Defects in Insulating Crystals, edited by F. Luty, University of Utah, 1984 (unpublished), p. 349.
[26]R. W. Dreyfus and A. S. Nowick, J. Appl. Phys. **33**, 473 (1962).
[27]D. L. Wood and W. Kaiser, Phys. Rev. **126**, 2079 (1962).
[28]K. Suzuki, J. Phys. Soc. Jpn. **16**, 67 (1961).
[29]G. H. Dieke and R. Sarup, J. Chem. Phys. **36**, 371 (1962).
[30]W. B. Gandrud and H. W. Moos, J. Chem. Phys. **49**, 2170 (1968).